https://doi.org/10.56801/MME1000

Analysis of Friction Stir Processed Surface Quality of AA2098 Aluminum Alloy for Aeronautical Applications

Mauro Carta[1], Pasquale Buonadonna[2], Gianluca Marongiu[3], Mohamad El Mehtedi[4]

[1]*Department of Mechanical, Chemical and Materials Engineering, University of Cagliari, Cagliari, Italy, mauro.carta94@unica.it*
[2,3,4]*Department of Mechanical, Chemical and Materials Engineering, University of Cagliari, Cagliari, Italy*

Received: 15-06-2023
Accepted: 16-08-2023

Abstract: FSP is a relatively new technique that changes the microstructure on the surface of the material to improve mechanical properties in the desired zone. This study aimed to investigate the surface quality of AA2098 sheets after being subjected to friction stir processing under different conditions of feed rate and rotational speed. A DoE analysis was developed with two factors, feed rate and rotational speed, and three different levels of 75, 100, 125 mm/min and 1000, 1250, 1500 rpm respectively, in order to assess the processed surface quality. The Sa parameter was used to represent the surface quality in different zones of the process, near entrance tool, middle and near exit tool, and ANOVA analysis was conducted. The results indicated that only the position and feed rate have a statistical influence on surface roughness. Additionally, the surface quality is strongly affected by the position relative to the entrance of the tool and the side (retreating or advancing sides). The roughness was found to be significantly lower on the advancing side rather than on the retreating side.

Keywords: Friction stir processing, surface quality, Design of Experiment, ANOVA.

1. Introduction

Friction stir welding (FSW) is a solid-state technique used to join samples together, which was first patented in 1991 by TWI (Cambridge, United Kingdom) [1]. Specifically, FSW of 2xxx Al-Cu aluminum alloys, such as AA2198, has gained widespread usage in fabricating lightweight structures requiring a high strength-to-weight ratio and good corrosion resistance. Many studies since then, have been carried out finding applications in different fields, particularly in the aeronautical sector [2, 3]. This research has also led to the development of novel techniques likes Friction stir extrusion (FSE), aimed at recycling light alloy machining chips for wire production [4]. Another innovation is Friction stir consolidation (FSC), employed to efficiently produce bulk material by processing of initially incoherent materials like recyclable chips or powders. The operational equipment for FSC closely mirrors that of FSE, differing only in the integration of an extrusion channel within the die. This innovative design enables the rotating tool not only to facilitate plastic deformation within the chamber but also to generate heat through friction, thereby further enhancing the overall process [5]. Friction stir

processing (FSP), developed by Mishra in 1999 [6], operates on the same principles as friction stir welding (FSW) but focuses on modifying the microstructure of specimen surfaces to improve their surface properties without joining samples. All process parameters can be categorized into machine variables, tool design variables, and material properties [7]. During the process, heating is generated through friction between the tool and the material's top surface. The rotating tool induces plastic flow in the metal, resulting in a stirred zone with fine grain structure in just a simple pass. Despite its potential advantages, FSP has not yet gain widespread adoption in industrial settings [8].

FSP was initially used to enhance the superplastic behavior by creating ultrafine-grained material (UFG) [6, 9]. An optimal range of modification process parameters plays an important role in achieving Ultra-Fine Grain (UFG) modification across a diverse variety array of parent metals. Various techniques can be utilized to obtain UFG, including the use of different tools, pin shapes, cooling procedures, and, nevertheless, Multipass techniques. In Multipass techniques, an increase in the number of passes leads to a gradual decrease in grain size, accompanied by a corresponding reduction in free dislocation density [10]. These passes can be carried out in parallel or perpendicular orientations. The incorporation of a cooling system allows for swift heat dissipation during the process, resulting in a significant reduction in grain size [11]. For processes involving a plate undergoing FSP, an innovative approach known as "submerged FSP" can be implemented. This involves the complete immersion of the plate within a liquid coolant, such as water. This innovation not only facilitates superior heat dissipation but also inhibits the growth of recrystallized grains. Flowing water is strategically employed to rapidly cool the plate immediately after the FSP tool's passage [12].

Moreover, the FSP process can also be adapted for use with a consumable material, known as friction stir alloying (FSA) or mechanical alloying, to generate metal matrix composites. FSA can enhance surface properties even more effectively than standard FSP, all while leaving the substrate properties unaffected [13-15]. Usage of ultrasonic vibrations during the process offers potential benefits, improving heat generating and material flow throughout the process [16].

As widely known, a majority of component failures initiate from the surface. Friction Stir Processing (FSP) presents the capability to enhance surface properties, including wear and corrosion resistance, hardness, strength, ductility, and fatigue life, precisely where needed, without affecting the substrate. The main aim of this study is to assess how operational factors, namely feed rate, and rotational speed, as well as the position of the treated zone, impact the resulting surface quality of the AA2098 plate after undergoing FSP. The selection of this alloy is driven by its significant relevance in aeronautical applications [17]. The evaluation of surface quality is conducted using the Sa parameter, with measurements taken from three distinct zones of the processed sample: near the entrance, middle, and near the exit of the tool.

While a previous study investigated the Sa parameter in FSP on AA2017 aluminum alloy [18], focusing on the effect of the normal force on Sa, this study's novelty lies in the utilization of a different alloy, AA2098, and its specific focus on examining the influence of position across a wide range of process parameter values.

2. Experimental procedure

The process of Friction Stir Processing (FSP) was carried out on a 5 mm thick AA2098-T351 aluminum alloy sheet utilizing a tool with a 17 mm shoulder diameter and a conic pin (as depicted in Figure 1a). Table 1 outlines the chemical composition of the alloy in terms of weight percentages. During the experiments, the tool was tilted at a 2° angle, and the process was executed using a CNC 5-axis milling machine, DECKEL MAHO - DMU 60P hi-dyn model. The experiments were randomized to eliminate potential external interactions.

A Design of Experiment (DoE) approach was adopted, involving two operational factors: rotational speed (n) and feed rate (Vf), both encompassing three different levels. The experimental design employed for the quality surface assessment was a full factorial design for both experimental setup and statistical analysis, as detailed in Table 2. The design incorporated three factors each with three distinct levels. A comprehensive schematic overview of the experimental methodology is illustrated in Figure 1c.

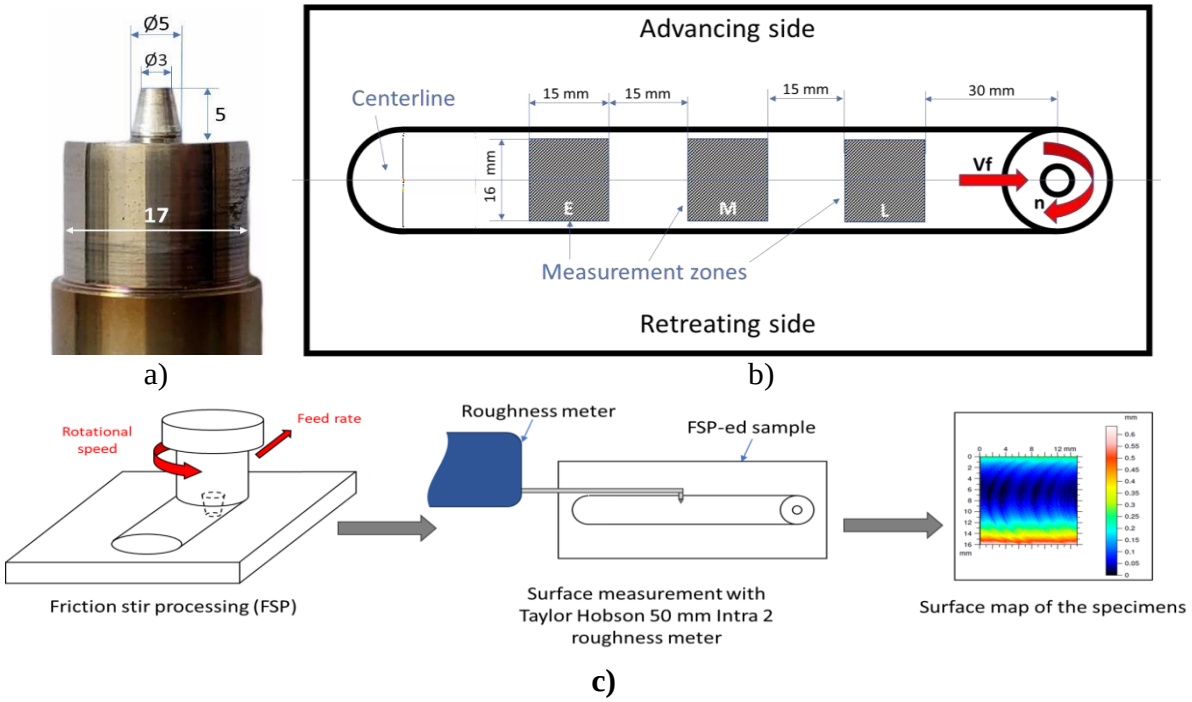

Figure. 1. a) Tool used for FSP, all measures in mm; b) Schematic representation of the measurements carry out on every sample; c) schematic overview of the experimental procedure.

Table 1. Chemical composition of the alloy (wt%).

Cu	Fe	Li	Mg	Mn	Si	Ag	Ti	Zn	Zr	Al
3.55	0.14	1.1	0.53	0.24	0.08	0.42	0.04	0.22	0.07	Bal.

Figure 1b shows an example of the resulting sample after FSP. The surface aspect appearance of a specimen that has undergone friction stir processing is characterized by typical semicircular streaks. The Sa parameter is a parameter used to describe the average roughness of a surface. It is defined as the Arithmetical Mean Height of the surface peaks, as shown below:

$$Sa = \frac{1}{A}\iint_A |Z(x,y)|dxdy \quad (1)$$

Table 2. Full factorial Design summary table.

Factors				Levels		
Name	**Type**	**Units**	**Symbols**	**1**	**2**	**3**
Rotational speed (n)	Numeric	[rpm]	A	1000	1250	1500
Feed Rate (Vf)	Numeric	[mm/min]	B	75	100	125
Position	Textual	[15]	C	E	M	L

To evaluate the influence of the position on the quality surface roughness across the FSPed zone, measurements were conducted on a 15 x 16 mm^2 surface area within three

designed zones: E, M and L (as illustrated in the scheme in Figure 2), using a Taylor Hobson 50 mm Intra 2 roughness meter for every condition.

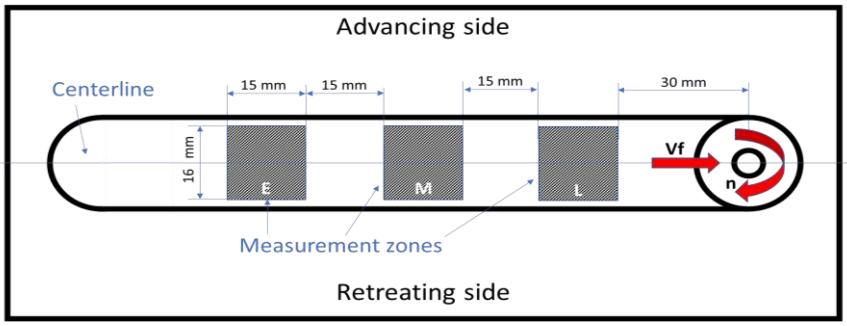

Figure 2. schematic representation of the Sa map measurements carry out for DoE analysis.

3. Results and discussion

Table 3 represents the complete set of Sa values obtained from the measurements. As previously indicated, these values are divided into three distinct zones: near the entrance, middle, and near the exit of the tool, as shown in Figure 2. The ANOVA tests were conducted using Sa as the response parameter. Figure 3 shows the Pareto chart demonstrating that among all variables, only two are statistically significant for the analysis: the feed rate and the position.

Table 3. Sa measured for each condition.

n [rpm]	Vf [mm/min]	Sa parameter [µm]					
		Advancing side			Retreating side		
		E	M	L	E	M	L
1000	75	3,01	3,85	5,49	3,25	5,42	6,06
1000	100	3,34	3,93	4,58	2,89	6,29	7,86
1000	125	4,48	4,57	7,61	4,89	8,3	5,79
1250	75	2,47	9,13	3,71	7,96	3,6	3,84
1250	100	3,56	3,25	4,27	2,88	3,92	6,66
1250	125	5,24	7,18	2,70	6,4	9,29	6,40
1500	75	3,33	4,35	5,25	4,09	4,68	5,00
1500	100	4,55	4,17	6,13	4,31	5,87	5,86
1500	125	3,49	4,11	7,47	3,59	7,19	6,35

The main effect plot for Sa demonstrates that the Sa parameter remains relatively constant within the selected range of the rotational speed, while it increases at higher level of feed rate. Moreover, there is a significant variation depending on the position of the measurement.

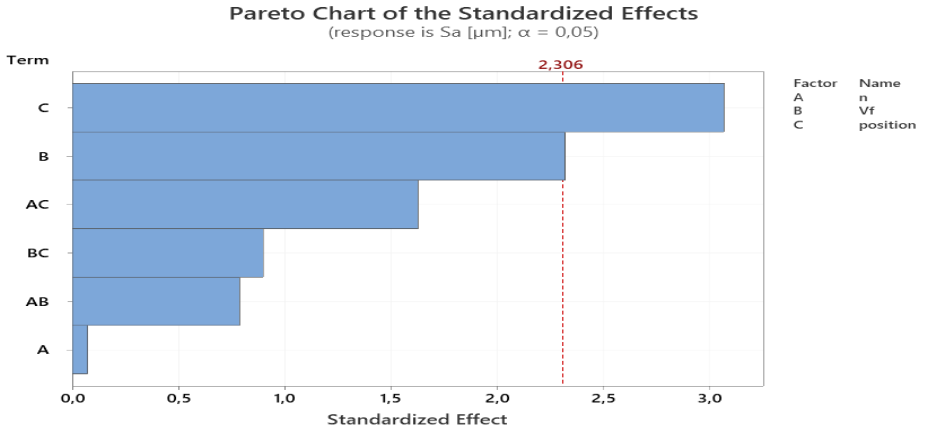

Figure 3. Pareto Chart of ANOVA Analysis.

The roughness consistently increases from the zone near the entrance of the tool to the middle zone and then slightly increases near the exit hole. The difference in roughness between the L-zone and M-zone is minimal, possibly indicating that the process has nearly reached a steady state at this point.

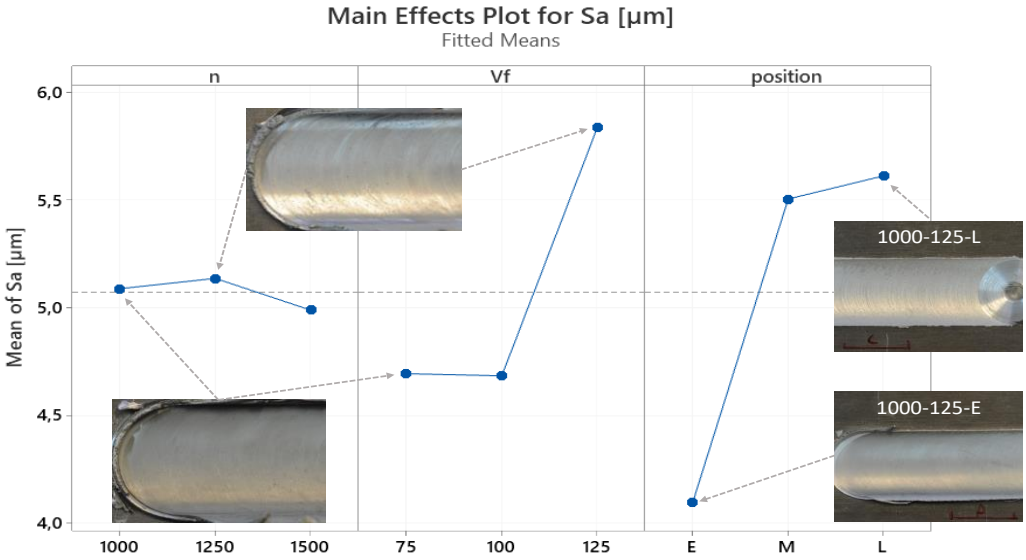

Figure 4. Main effect plot for Sa.

To better investigate the results regarding the position, the surface measurements were divided into two distinct zones based on the centerline along the process. This division resulted in two separate surfaces for each measurement, corresponding to the retreating and advancing sides. Table 3 presents all the Sa values obtained from this evaluation, encompassing a total of six zones: near the entrance, middle, and near the exit of the tool, each divided into retreating and advancing zones.

ANOVA test has been evaluated again with the data reported in Table 3. Therefore, we have three factors: rotational speed, feed rate, and position of measurement, with three levels, three levels, and six levels respectively. The results are reported in Table 4 and plotted in Figure 5.

Table 4. Analysis of Variance for Sa parameter.

Factor	Degrees of Freedom	Sum of squares	Mean Square	F-Value	P-Value
n	2	0,205	0,1024	0,06	0,940
Vf	2	15,793	7,8964	4,83	0,019
position	5	36,324	7,2648	4,44	0,007
n*Vf	4	7,135	1,7838	1,09	0,388
n*position	10	34,826	3,4826	2,13	0,072
Vf*position	10	29,578	2,9578	1,81	0,124
Error	20	32,706	1,6353		
Total	53	156,567			

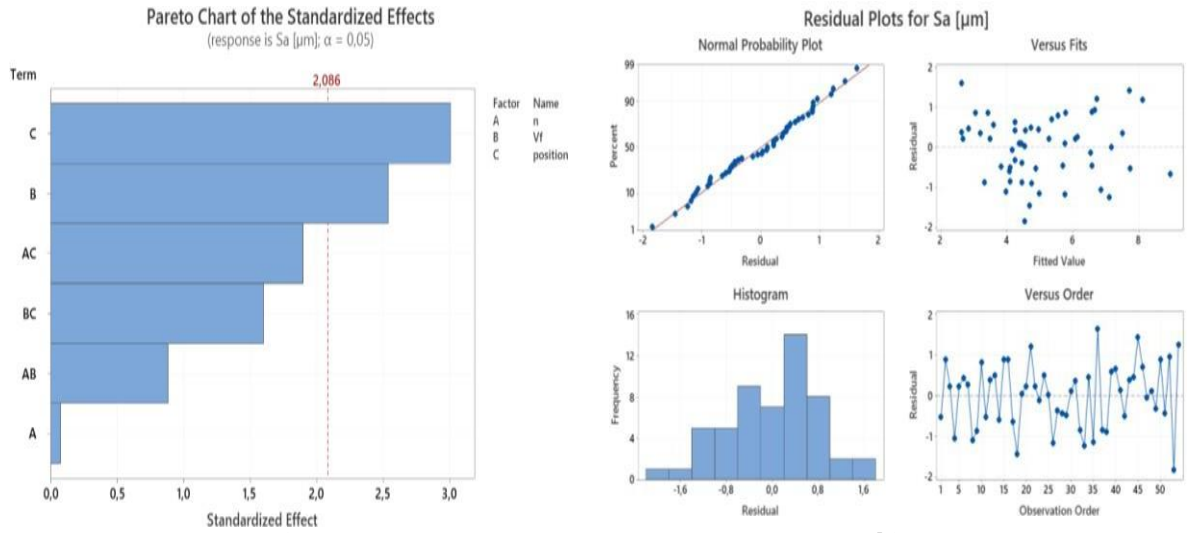

a) b)

Figure. 5. a) Pareto Chart and b) Residual plots for Sa.

Table 4 displays the results of the ANOVA analysis for each coefficient, which have been evaluated and tested at a 95% confidence level. This analysis demonstrated that, there were statistically significant variations observed among the tested samples, based on factors such as rotational speed (n), feed rate (Vf), position, and their 2-way interactions. In particular, just Vf and position have a p-value under 0.05, which means that have a statistical influence on Sa response.

From the Pareto Chart in Figure 5a, it is evident that, once again, only position and feed rate have a statistically significant influence on the Sa parameter.

Figure 5b presents the residual plots for surface roughness. The normal plot demonstrates that the majority of the points are closely aligned with the mean line, indicating that the data is approximately normally distributed. Furthermore, thorough examination of the plot versus fits, histogram, and versus order did not reveal any discernible patterns or anomalous structures within the data.

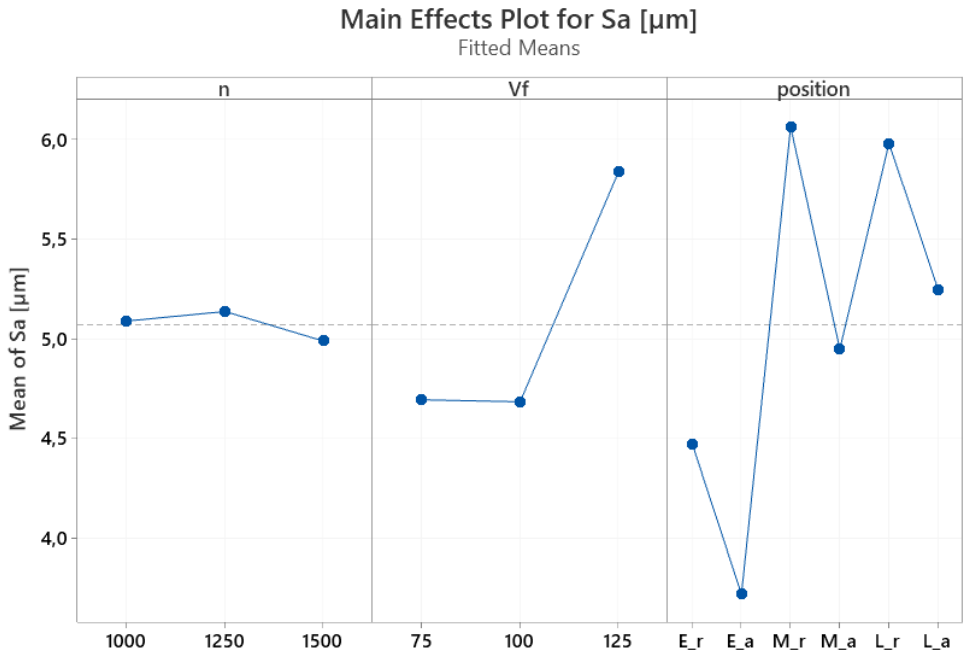

Figure 6. Main effect plot and Interaction plot for Sa.

The main effect plots depict the influence of each factor on the Sa parameter response. It is noteworthy that the Sa parameter remains relatively constant as the rotational speed varies within the selected range. This observation is supported by the ANOVA results and the Pareto Chart, which indicate that rotational speed does not have a statistically significant effect on surface roughness. However, it is worth mentioning that using higher rotational speeds is preferable to achieve the desired deformation temperature. In terms of the feed rate (Vf), the Sa parameter remains relatively constant from the lower to the middle level. However, it increases at the higher feed rate level, similar to the findings observed in the previous case. Notably, interesting results have been obtained for the position factor, demonstrating that the Sa parameter is lower on the advancing side compared to the corresponding zone on the retreating side.

In particular, on the advancing side the roughness increases from the zone near the entrance of the tool (E) to the exit (L), while on the retreating side a remarkable increase can be observed from the E-zone to the M-zone, while the difference between the L-zone and the M-zone is not substantial, with a light decrease in roughness. On both sides the difference between the L-zone and the M-zone is not significant, which probably means that the FSP at this point has almost reached a steady state.

4. Conclusions

In summary, this study examined the impact of feed rate and rotational speed on the surface quality of AA2098 sheets that underwent friction stir processing. Sa parameter was used as representative parameters of surface quality, and the data were analyzed using Minitab software and ANOVA techniques. The results of the study revealed that surface roughness was significantly influenced by two factors: feed rate and position. Specifically, the position of the material relative to the tool entrance and whether it was on the retreating or advancing side had a profound impact on surface quality. Notably, the roughness on the advancing side was significantly lower compared to the retreating side. Moreover, it was observed that increasing the feed rate beyond 100 mm/min resulted in a deterioration of surface quality, leading to unfavorable mechanical properties. Additionally, in position E (the initial processed part), the surface quality consistently exhibited better results compared to the L zone across all investigated conditions. These findings provide valuable insights for optimizing friction stir processing parameters and emphasize the importance of selecting an appropriate feed rate to achieve superior surface quality in AA2098 sheets.

5. Funding Details

This research received co-financing of the European Union - FESR o FSE, PON Research & Innovation 2014-2020.

References

1. Bitondo, C., et al., *Friction stir welding of AA2198-T3 butt joints for aeronautical applications.* International Journal of Material Forming, 2010. **3**: p. 1079-1082.
2. Bitondo, C., et al., *Friction-stir welding of AA 2198 butt joints: mechanical characterization of the process and of the welds through DOE analysis.* The International Journal of Advanced Manufacturing Technology, 2011. **53**: p. 505-516.
3. Velotti, C., et al., *FSW of AA 2139 plates: Influence of the temper state on the mechanical properties.* Key Engineering Materials, 2013. **554**: p. 1065-1074.

4. El Mehtedi, M., et al., *A new sustainable direct solid state recycling of AA1090 aluminum alloy chips by means of friction stir back extrusion process.* Procedia CIRP, 2019. **79**: p. 638-643.
5. Baffari, D., et al. *Bonding prediction in friction stir consolidation of aluminum alloys: A preliminary study*. in *AIP Conference Proceedings*. 2018. AIP Publishing.
6. Mishra, R.S., et al., *High strain rate superplasticity in a friction stir processed 7075 Al alloy.* Scripta materialia, 1999. **42**(2): p. 163-168.
7. Dubey, M.K. and G. Deep, *Investigation of the process parameter and their influence on the mechanical properties of friction stir processed surface composite: a review.* International Journal of Applied Engineering Research, 2018. **13**(9): p. 75-82.
8. Węglowski, M.S., *Friction stir processing—state of the art.* Archives of civil and Mechanical Engineering, 2018. **18**: p. 114-129.
9. Li, K., X. Liu, and Y. Zhao, *Research status and prospect of friction stir processing technology.* Coatings, 2019. **9**(2): p. 129.
10. Ramesh, K., S. Pradeep, and V. Pancholi, *Multipass friction-stir processing and its effect on mechanical properties of aluminum alloy 5086.* Metallurgical and Materials Transactions A, 2012. **43**: p. 4311-4319.
11. Yazdipour, A. and K. Dehghani, *Modeling the microstructural evolution and effect of cooling rate on the nanograins formed during the friction stir processing of Al5083.* Materials Science and Engineering: A, 2009. **527**(1-2): p. 192-197.
12. Liu, F., et al., *Microstructural evolution and superplastic behavior in friction stir processed Mg–Li–Al–Zn alloy.* Journal of materials science, 2013. **48**: p. 8539-8546.
13. Rastabi, S.A. and M. Mosallaee, *Effects of multipass friction stir processing and Mg addition on the microstructure and tensile properties of Al 1050 alloys.* International Journal of Minerals, Metallurgy and Materials, 2022. **29**: p. 97-107.
14. Teo, G.S., K.W. Liew, and C.K. Kok, *A Study on Friction Stir Processing Parameters of Recycled AA 6063/TiO2 Surface Composites for Better Tribological Performance.* Metals, 2022. **12**(6): p. 973.
15. Zayed, E.M., et al., *Development and characterization of AA5083 reinforced with SiC and Al 2 O 3 particles by friction stir processing.* Engineering design applications, 2019: p. 11-26.
16. Kumar, S., *Ultrasonic assisted friction stir processing of 6063 aluminum alloy.* Archives of Civil and Mechanical Engineering, 2016. **16**: p. 473-484.
17. Hajjioui, E.A., et al., *A review of manufacturing processes, mechanical properties and precipitations for aluminum lithium alloys used in aeronautic applications.* Heliyon, 2022.
18. Langlade, C., et al. *Influence of friction stir process parameters on surface quality of aluminum alloy A2017*. in *MATEC web of conferences*. 2017. EDP Sciences.